Nitric oxide signaling controls collective contractions in a colonial choanoflagellate

Josean Reyes-Rivera, Yang Wu, Benjamin G.H. Guthrie, Michael Marletta, Nicole King, Thibaut Brunet

Report

Current Biology

Nitric oxide signaling controls collective contractions in a colonial choanoflagellate

Highlights

- The choanoflagellate *C. flexa* encodes a complete nitric oxide signaling pathway
- *C. flexa* responds to NO by contractions resulting in a feeding-to-swimming switch
- NO binds *C. flexa* soluble guanylate cyclase 1 (*Cf* sGC1) and induces cGMP synthesis
- sGC activity maintains NO-induced contractions

Authors

Josean Reyes-Rivera, Yang Wu, Benjamin G.H. Guthrie, Michael A. Marletta, Nicole King, Thibaut Brunet

Correspondence

marletta@berkeley.edu (M.A.M.), nking@berkeley.edu (N.K.), thibaut.brunet@pasteur.fr (T.B.)

In brief

Although nitric oxide signaling regulates key physiological processes in animals, its premetazoan origin is unclear. Reyes-Rivera et al. report a full animal-like NO signaling pathway in a close outgroup to animals, the multicellular choanoflagellate *Choanoeca flexa*, in which NO induces contractions, resulting in a switch from feeding to swimming.

Reyes-Rivera et al., 2022, Current Biology *32*, 2539–2547
June 6, 2022
https://doi.org/10.1016/j.cub.2022.04.017

CellPress

Current Biology

CellPress
OPEN ACCESS

Report

Nitric oxide signaling controls collective contractions in a colonial choanoflagellate

Josean Reyes-Rivera,[1] Yang Wu,[2] Benjamin G.H. Guthrie,[2] Michael A. Marletta,[2,*] Nicole King,[1,*] and Thibaut Brunet[3,4,*]
[1]Howards Hughes Medical Institute and the Department of Molecular and Cell Biology, University of California, Berkeley, Berkeley, CA, USA
[2]Department of Chemistry and the Department of Molecular and Cell Biology, University of California, Berkeley, Berkeley, CA, USA
[3]Institut Pasteur, Université Paris-Cité, Department of Cell Biology and Infection, and the Department of Developmental and Stem Cell Biology, 75015 Paris, France
[4]Lead contact
*Correspondence: marletta@berkeley.edu (M.A.M.), nking@berkeley.edu (N.K.), thibaut.brunet@pasteur.fr (T.B.)
https://doi.org/10.1016/j.cub.2022.04.017

SUMMARY

Although signaling by the gaseous molecule nitric oxide (NO) regulates key physiological processes in animals, including contractility,[1–3] immunity,[4,5] development,[6–9] and locomotion,[10,11] the early evolution of animal NO signaling remains unclear. To reconstruct the role of NO in the animal stem lineage, we set out to study NO signaling in choanoflagellates, the closest living relatives of animals.[12] In animals, NO produced by the nitric oxide synthase (NOS) canonically signals through cGMP by activating soluble guanylate cyclases (sGCs).[13,14] We surveyed the distribution of the NO signaling pathway components across the diversity of choanoflagellates and found three species that express NOS (of either bacterial or eukaryotic origin), sGCs, and downstream genes previously shown to be involved in the NO/cGMP pathway. One of the species coexpressing sGCs and a bacterial-type NOS, *Choanoeca flexa*, forms multicellular sheets that undergo collective contractions controlled by cGMP.[15] We found that treatment with NO induces cGMP synthesis and contraction in *C. flexa*. Biochemical assays show that NO directly binds *C. flexa* sGC1 and stimulates its cyclase activity. The NO/cGMP pathway acts independently from other inducers of *C. flexa* contraction, including mechanical stimuli and heat, but sGC activity is required for contractions induced by light-to-dark transitions. The output of NO signaling in *C. flexa*—contractions resulting in a switch from feeding to swimming—resembles the effect of NO in sponges[1–3] and cnidarians,[11,16,17] where it interrupts feeding and activates contractility. These data provide insights into the biology of the first animals and the evolution of NO signaling.

RESULTS

C. flexa encodes both NOS and sGC

C. flexa is a colonial choanoflagellate that forms concave sheets capable of global inversion of their curvature through collective contractility.[15] *C. flexa* inversion mediates a trade-off between feeding and swimming: relaxed colonies (with their flagella pointing inside) are slow swimmers and efficient feeders, whereas contracted colonies (with their flagella pointing outside) are inefficient feeders but fast swimmers[15] (Figure 1A). Inversion has been shown to be induced by light-to-dark transitions through the inactivation of a rhodopsin phosphodiesterase (Rho-PDE) and accumulation of cyclic guanosine monophosphate (cGMP)[15] (Figure 1B). The involvement of cGMP in collective contraction in *C. flexa* and the connection between nitric oxide (NO)/cGMP signaling and tissue contraction in nonbilaterian animals[18] led us to investigate whether NO signaling might exist and regulate sheet inversion in *C. flexa* (Figure 1B).

By examining the genomes of two choanoflagellates (*Monosiga brevicollis*[19] and *Salpingoeca rosetta*[20]) and the transcriptomes of *C. flexa*[15] and 19 other choanoflagellates,[21] we found that five choanoflagellate species encode nitric oxide synthase (NOS) homologs and that nine choanoflagellate species encode soluble guanylate cyclase (sGC) homologs (Figure 2A). Of these, three species—*Salpingoeca infusionum*, *Choanoeca perplexa*, and *C. flexa*—express both NOS and sGCs, suggesting that some aspect of the physiology of these organisms might be regulated by NO/cGMP signaling.

Like metazoan NOS genes, choanoflagellate NOS genes encode the canonical oxygenase and reductase domains (Figure 2B). Phylogenetic analysis revealed that one choanoflagellate NOS gene, from *S. infusionum*, is closely related to those from metazoans and fungi (Figure S1A). In contrast, all other choanoflagellate NOSs (including those from *C. flexa*) cluster with cyanobacterial NOSs, suggesting that they might have been acquired through horizontal gene transfer from a cyanobacterial ancestor early in the evolution of choanoflagellates (Figure S1A). Current uncertainties surrounding the choanoflagellate phylogeny[12,22] make it difficult to pinpoint exactly when this horizontal gene transfer event occurred and whether it followed or preceded the loss of the ancestral eukaryotic NOS in most or all choanoflagellates. These choanoflagellate NOS

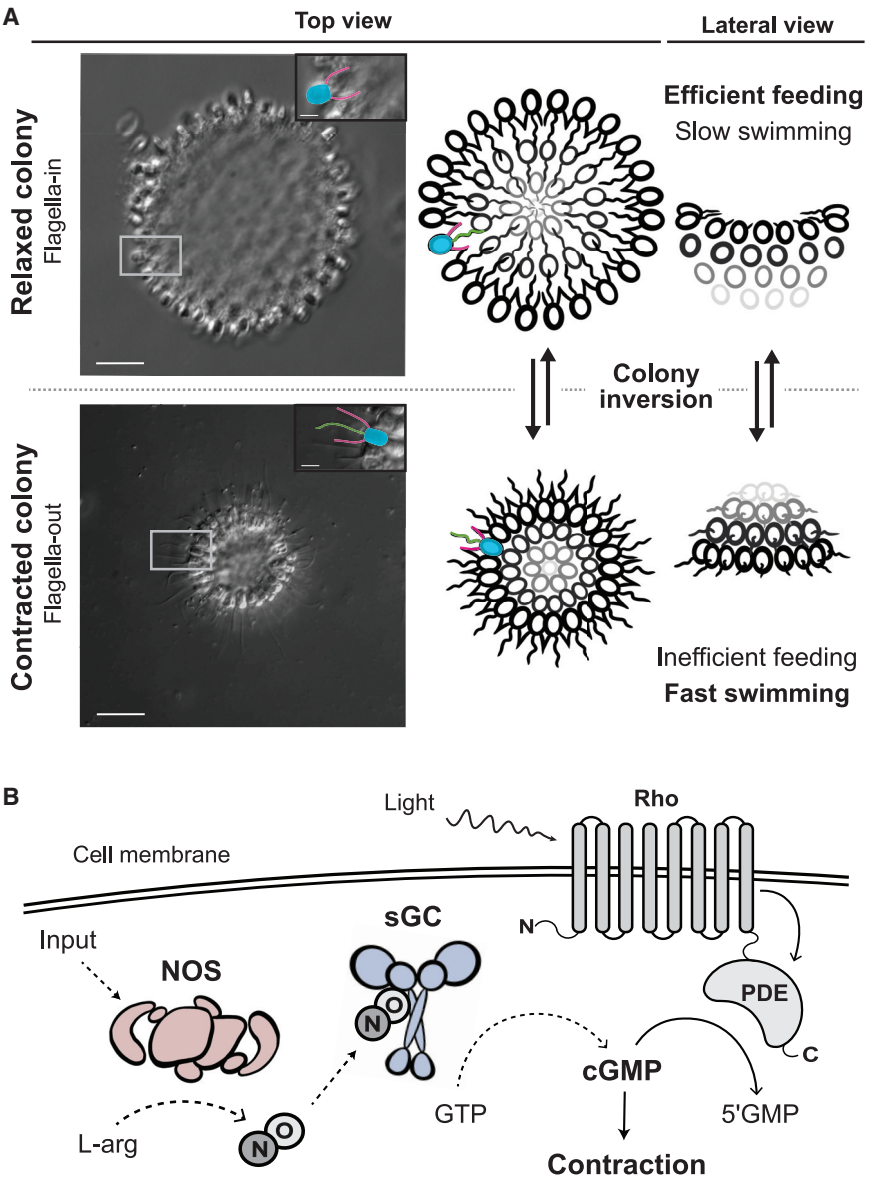

Figure 1. The inversion behavior of *C. flexa*, its control by light, and hypothesized control by NO

(A) Micrograph (left) and schematic depiction (right) of *C. flexa* inversion behavior. Cells are linked by their collars and form a cup-shaped monolayer or sheet; scale bars, 15 μM. Relaxed colonies (top half) have their flagella pointing toward the inside of the colony and are efficient feeders and slow swimmers. (Flagella from relaxed colony are not in focus in the micrograph; see schematic for flagellum orientation.) Contracted colonies (bottom half) have their flagella pointing toward the outside of the colony and are inefficient feeders but fast swimmers. Insets: pseudocolors highlight the characteristic morphological features of choanoflagellates: flagella (green), cell body (blue), and microvilli (magenta). Inset scale bars, 5 μm.

(B) *C. flexa* colony inversion is controlled by light-to-dark transitions, mediated by a rhodopsin-phosphodiesterase fusion protein (Rho-PDE) upstream cGMP signaling. In the presence of light, Rho-PDE is active and constantly converting cGMP into 5′GMP. We hypothesized that NO/cGMP signaling might also be able to induce inversion. Mechanisms tested in this paper are indicated with dashed lines: a primary input activates the nitric oxide synthase (NOS), which converts L-arginine into NO and L-citrulline. NO diffuses away and activates soluble guanylate cyclase (sGC) that convert GTP into cGMP, causing colony contraction.

genes, like those of cyanobacteria, differ from metazoan NOS, in which they encode an upstream globin domain with unknown function and lack the calmodulin-binding domain that mediates regulation of metazoan NOSs by Ca^{2+}, suggesting that calcium signaling does not regulate NO synthesis in *C. flexa*. The *C. flexa* transcriptome also encodes complete biosynthetic pathways for the NOS cofactors tetrahydrobiopterin (BH_4), flavin mononucleotide (FMN), flavin adenine dinucleotide (FAD), and nicotinamide dinucleotide phosphate (NADPH) (Figure S2A) as well as downstream genes in the NO/cGMP signaling pathway: cGMP-dependent kinase (PKG), cGMP-gated ion channels (CNG), and cGMP-dependent PDE (PDEG) (Figure S2B), providing additional evidence that *C. flexa* employs NO signaling as part of its physiology.

Nearly all sGC genes from choanoflagellates, including *C. flexa*, encode the canonical domains observed in animal sGCs: the heme NO-/O_2-binding domain (HNOB or H-NOX), the HNOB-associated domain (HNOBA), and the C-terminal catalytic domain (guanylate cyclase)[23] (Figure 2C). Phylogenetic analysis revealed that all animal and most choanoflagellate sGCs (including those of *C. flexa*) evolved from a single ancestral sGC found in the last common ancestor of choanoflagellates and metazoans that diversified separately into multiple paralogs in these two lineages (Figure S1B). In contrast, the predicted sGC from one choanoflagellate species, *S. helianthica*, more closely resembles the sGCs of chlorophyte algae (which are the only protist group previously known to encode sGC proteins with a metazoan-like domain architecture[24]; Figure S1B).

Importantly, not all animal sGCs are regulated by NO: in *Drosophila melanogaster* and *Caenorhabditis elegans*, the so-called "atypical sGCs" preferentially bind soluble O_2 instead of NO and are thought to be involved in the regulation of feeding by oxygen concentration.[25–27] Discrimination between NO and O_2 is mediated by the presence of a hydrogen-bonding network, where a distal pocket tyrosine residue is critical for stabilizing the heme-O_2 complex.[28] We generated preferential binding predictions based on this motif[28,29] and found that both NO- and O_2-preferential binding sGCs are widely distributed among choanoflagellates with no obvious pattern (Figures 2A and S2D). Interestingly, predicted NO-selective

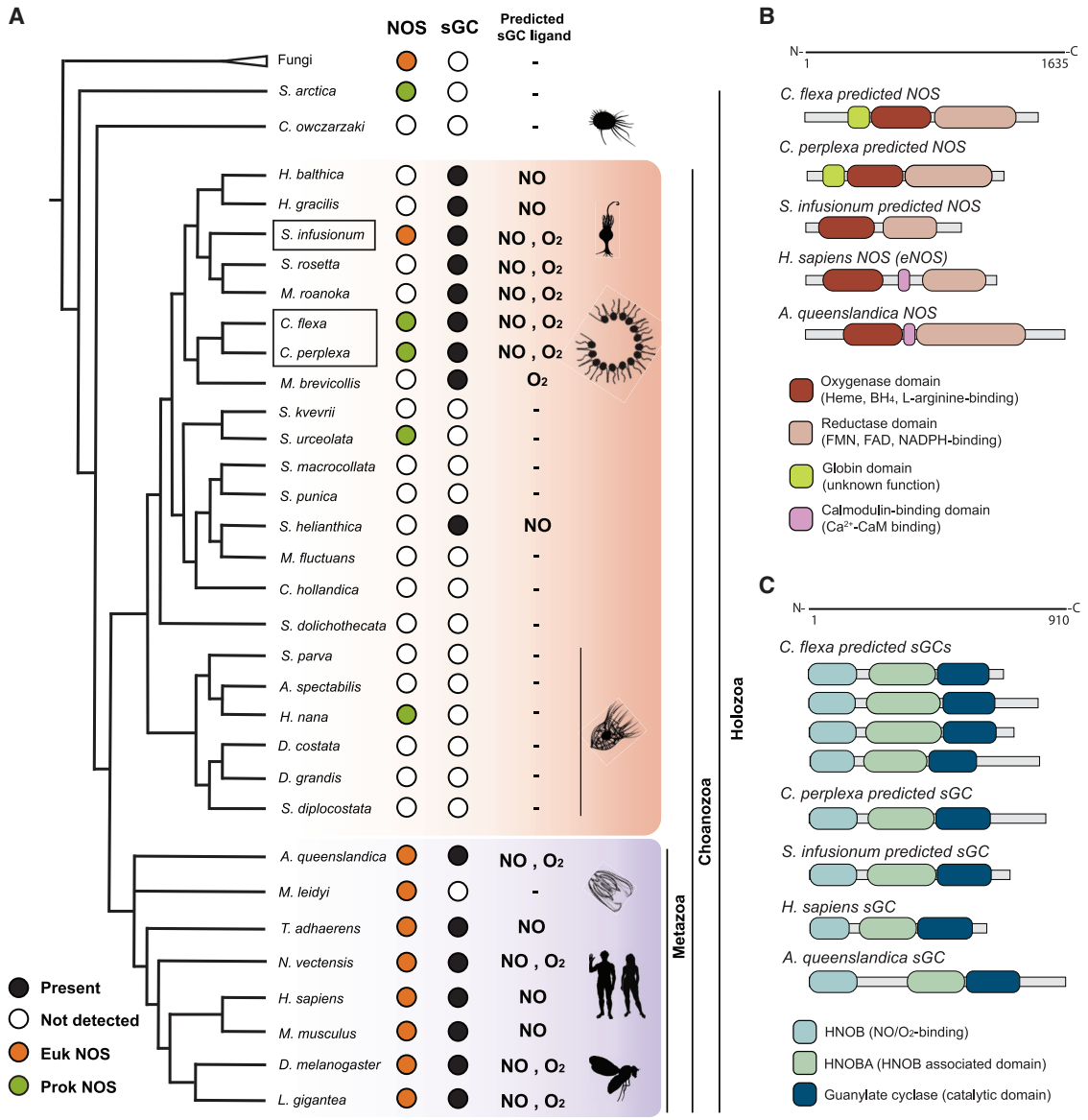

Figure 2. NO synthase (NOS) and soluble guanylate cyclases (sGCs) predicted to bind either NO or O_2 are broadly distributed across choanozoans, and all three are present in *C. flexa*

(A) Phylogenetic distribution of NOS and sGC across opisthokonts. *C. flexa*, its sister species *C. perplexa*, and *S. infusionum* encode both NOS and NO-sensitive sGCs, as do animals.

(B) Choanoflagellate NOSs have the metazoan canonical oxygenase and reductase domain but lack the calcium-calmodulin binding domain. *C. flexa* and other choanoflagellate NOS encode an upstream globin domain with unknown function, also observed in cyanobacterial NOS.

(C) *C. flexa* sGCs have the same domain architecture as animal sGCs. See Figure S1 for phylogenetic analysis and Figure S2 for phylogenetic distribution of NO/cGMP downstream components.

sGCs are present in choanoflagellate species in which NOS was not detected, suggesting that these species might detect NO from an exogenous source (i.e., environmental bacteria or other protists), might possess an alternative NO-producing mechanism, or might encode an NOS that was not detected in the transcriptome. In *C. flexa*, one of the four sGC transcripts was predicted to be selective for NO and was named *Cf* sGC1 (Figure S2D). The other two choanoflagellate species found to possess both an NOS and sGCs, *C. perplexa* and *S. infusionum*, were also predicted to encode at least one NO-sensitive sGC (Figure 2A).

NO/cGMP signaling controls colony contraction in *C. flexa*

To test whether NO signaling regulates collective contractions in *C. flexa*, we treated *C. flexa* cultures with several NO donors,[30] compounds capable of releasing NO in solution. We found that treatment of *C. flexa* with the NO donors proliNONOate and

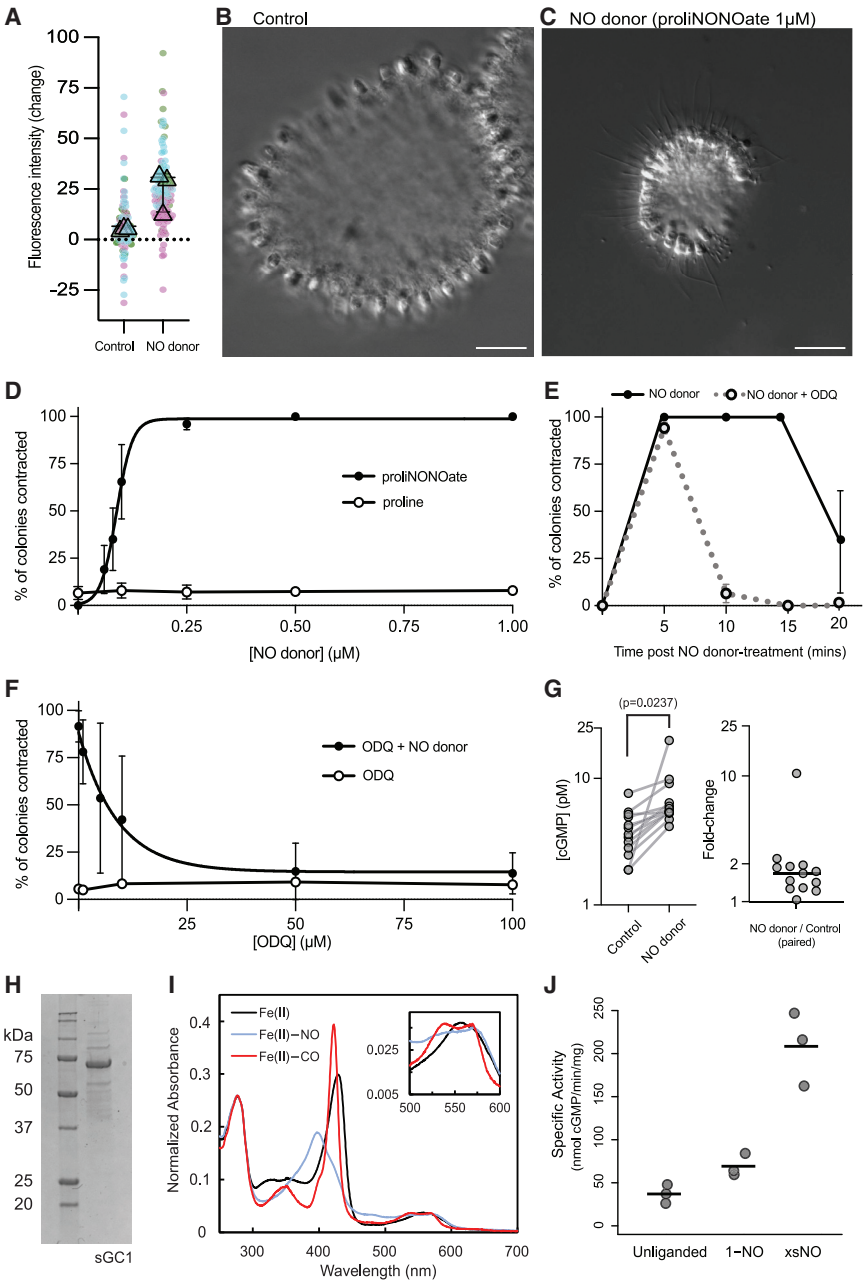

Figure 3. NO induces sustained colony contraction in *C. flexa* and activates *Cf* sGC1

(A) NO release by proliNONOate was visualized by loading cells with the NO-sensitive fluorescent probe DAF-FM and measuring the change in intracellular fluorescence intensity over 30 min. Cells treated with NO donor showed a higher increase in fluorescence. Graph is a SuperPlot[31] of n = 3 biological replicates per condition, with sample sizes N = 27, 33, and 47 for the three control groups and N = 26, 57, and 42 for the three treated groups. p = 0.0331 by an unpaired t test. See Figures S3A–S3C for a similar analysis using the NO donor DEANONOate.

(B and C) NO induces colony contraction. Although colonies treated with a negative control compound (proline) remained relaxed, colonies treated with 0.25 μM of the NO donor proliNONOate contracted within 1–2 min.

(D) The NO donor proliNONOate induces contractions within ~1–2 min in a dose-dependent manner. A closely related molecule incapable of releasing NO (proline) had no effect over the same concentration range. Figure S3D shows NO-induced contractions using different NO donors. Error bars indicate standard deviations.

(E) Inhibition of sGCs with 50 μM ODQ did not abolish NO-induced contraction at early time points but greatly reduced its duration. ODQ-treated colonies were contracted within 5 min post-treatment with NO donor but relaxed soon after, whereas untreated colonies remain contracted for at least 5 more min. Error bars indicate standard deviations.

(F) Inhibition of sustained contraction by ODQ is dose dependent. Colonies were incubated with different concentrations of ODQ for 1 h before treatment with 0.25 μM of the NO donor proliNONOate. We quantified the percentage of contracted colonies 10 min after NO treatment. In (D–F), each point represents the mean value of n = 3 biological replicates with at least 30 colonies scored per biological replicate. Error bars are standard deviations.

(G) Treatment of cells with a NO donor increased intracellular cGMP concentration almost 2-fold as quantified by ELISA. N = 13 pairs of control/treated samples, p = 0.024 by a paired t test.

(H–J) Purification, ligand binding properties, and specific activity of *Cf* sGC1. (H) Coomassie-stained SDS-PAGE gel of recombinant *Cf* sGC1 expressed in *E. coli* and purified. Band in lane "sGC1" represents *Cf* sGC1 with a monomeric molecular weight of 75.7 kDa. Left lane, molecular weight ladder. (I) UV-visible absorption spectra of *Cf* sGC1 under unliganded (black), NO-bound (blue), and CO-bound (red) conditions. Soret maxima: NO-bound: 429 nm; CO-bound: 423 nm; NO-bound: 399 nm. Inset, α/β bands show increased splitting upon ligand binding. (J) Specific activity of *Cf* sGC1 under unliganded, equimolar quantities of NO (1-NO) and excess NO (xsNO) conditions. Initial rates were measured from activity assays performed at 25°C, pH 7.5 with 1.5 mM Mg^{2+}-GTP substrate and 40 nM enzyme. Horizontal bars represent mean of three biological replicates.

DEANONOate led to an increase in intracellular NO as detected by the NO-sensitive fluorescent probe 4-Amino-5-Methylamino-2',7'-Difluorofluorescein (DAF-FM), demonstrating that they could be effective reagents for studying NO signaling in *C. flexa in vivo* (Figures 3A and S3A–S3C). Treatment of *C. flexa* with proliNONOate (Figures 3B and 3C) induced colony contraction within 1–2 min (although the inversion process itself only lasted a few seconds, as previously described for darkness-induced inversion[15]; see Video S1). The inversion response of *C. flexa* to proliNONOate was concentration dependent (Figure 3D), reaching a plateau of nearly 100% inversion at a concentration of 0.1 μM. As a negative control, *C. flexa* did not invert in response to proline, the molecular backbone of proliNONOate and the end product of NO release (Figure 3D). Moreover,

treatment with two other NO donors, DEANONOate or NOC-12, also induced inversion (Figure S3D). Taken together, these results indicate that NO is sufficient to induce colony contraction.

We next investigated whether NO triggers cGMP synthesis in *C. flexa*. We found that a pan-inhibitor of sGCs, oxadiazolo-quinoxalin-1-one (ODQ),[32] had no detectable effect on the percentage of contracted colonies 5 min after treatment with NO relative to cultures not treated with ODQ. However, a difference between the two conditions became evident 10 min after NO treatment, with nearly all ODQ-treated colonies relaxing into the uncontracted form, although all ODQ-untreated colonies remained contracted at least twice as long (Figure 3E). This premature relaxation of ODQ-treated colonies was concentration dependent (Figure 3F).

These results suggest that the maintenance of NO-induced colony contraction requires sGC activity. However, the pan-sGC inhibitor ODQ does not allow us to discriminate between NO- and O_2-sensitive sGCs. If NO does indeed signal through the sGC/cGMP pathway, we predicted that treatment of colonies with an NO donor should increase intracellular cGMP concentration. We found that NO-treated cells contained consistently higher intracellular cGMP levels than untreated cells (~2-fold increase on average, $p = 0.0237$; Figure 3G). Importantly, prior work has demonstrated that treatment of *C. flexa* with a cell-permeant form of cGMP (8-Br-cGMP) is sufficient to induce inversion.[15] These results further support the hypothesis that NO activates sGCs and stimulates the production of cGMP, which might contribute to maintaining *C. flexa* colony contraction.

C. flexa sGC1 is an NO-selective and catalytically active component of the *C. flexa* NO/cGMP signaling pathway

Of the four sGCs expressed by *C. flexa*, only one (*Cf* sGC1) was predicted to be selective for NO (Figure 1A). To directly test the existence of a canonical NO/sGC/cGMP pathway in *C. flexa*, we characterized ligand binding and activity of *Cf* sGC1 that had been heterologously expressed in and purified from *E. coli* (Figure 3H). The ligand specificity of sGCs can be determined by comparing the "Soret peak" maxima of the ultraviolet-visible (UV-vis) absorption after incubation with different gases, including NO, O_2, or CO. The Fe(II), unliganded form of *Cf* sGC1, exhibited a Soret peak at 429 nm and a single broad plateau in the α/β region (500–600 nm), consistent with that of an NO-selective sGC[29] (Figure 3I; Table S1). In the presence of NO, the Soret peak shifted to 399 nm with two peaks in the α/β region, as characteristic for a 5-coordinate, high-spin NO-heme complex[29] (Figure 3I; Table S1). On the other hand, when exposed to atmospheric oxygen in the absence of NO, the UV-vis absorption spectrum of *Cf* sGC1 did not change (Figures 3I and S4B), consistent with our prediction that *Cf* sGC1 is an NO-selective sGC and does not bind O_2. Moreover, like previously characterized animal sGCs, *Cf* sGC1 also binds CO to form a 6-coordinate, low-spin CO-heme complex,[33] evidenced by a Soret band maximum of 424 nm with two peaks in the α/β region (Figure 3I; Table S1). Thus, the UV-vis spectroscopy results indicate that *Cf* sGC1 binds diatomic gas ligands in a manner that resembles other well-characterized NO-selective sGCs. Finally, size exclusion chromatography showed that *Cf* sGC1 formed a homodimer (Figure S4A), similar to the dimeric structure of animal sGCs.

In animals, NO-selective sGCs display three levels of activity: (1) in the absence of NO, the protein has a low basal guanylate cyclase activity; (2) when one NO molecule is bound at the heme moiety, the protein is partially activated (to several-fold the basal activity); and (3) in the presence of excess NO, the protein reaches maximal activation.[34] To characterize the enzymatic activity of Cf sGC1, we measured cGMP production by purified *Cf* sGC1 under unliganded, equimolar NO, and excess NO conditions using an endpoint activity assay. We found that *Cf* sGC1 has an activity profile similar to that of animal sGCs, with a 2-fold increase in activity under equimolar NO concentration and ~6-fold increase under excess NO (Figure 3J). Overall, *Cf* sGC1 exhibits similar ligand binding properties and NO-stimulated activity profile to animal NO-specific sGCs.[33] These results further support the existence of NO/cGMP signaling in *C. flexa* and is consistent with it being mediated (at least in part) by *Cf* sGC1.

NO/cGMP signaling acts independently from most other inducers of colony contraction

In animals, NO signaling can be induced by a broad range of stimuli, which include chemical signals (for example, acetylcholine in mammalian blood vessels[35]), mechanical cues (for example, shear stress in blood vessels[36]), or heat shocks.[37–40] Interestingly, collar contractions in choanoflagellates can often be induced by mechanical stimuli, such as flow and touch.[41–44] We thus set out to test whether NO signaling in *C. flexa* responds to or intersects with environmental inducers of inversion.

We observed that *C. flexa* colonies invert in a matter of seconds in response to agitation of culture flasks (which presumably combines the effect of flow and shocks with other colonies or the walls of the flask) and to heat shocks (Figures 4A and 4B). To test whether mechanically or heat-induced contraction requires NO/cGMP signaling, we incubated the colony cultures with the pan-sGC inhibitor ODQ and exposed them to either of the two different stressors. We found that the inhibition of sGCs did not abolish mechanically induced or heat shock-induced contraction (Figures 4A and 4B). Taken together, these findings suggest that the mechanosensitive and thermosensitive pathways that induce inversion in *C. flexa* are independent of sGCs and hint at complex behavioral regulation in this choanoflagellate.

Previous work has shown that *C. flexa* colonies invert in response to light-to-dark transitions that they detect through a Rho-cGMP pathway.[15] In the presence of light, a Rho-PDE hydrolyzes cGMP into 5′-GMP, thus preventing cGMP signaling. In darkness, the Rho-PDE is inactivated, which allows cGMP to accumulate and trigger colony inversion (Figure 1B). Interestingly, this pathway requires the presence of cGMP, which is presumably synthesized by either particulate (i.e., membrane bound) or soluble (i.e., cytosolic) guanylate cyclases,[45] both of which are predicted to be encoded by the *C. flexa* transcriptome (Figure S2C). A third family of guanylate cyclases—NIT-GCs, recently discovered in animals—could not be detected in choanoflagellates.[46]

We next set out to answer whether sGCs are necessary for synthesizing the cGMP required for phototransduction. To address this, we treated light-sensitive colonies with ODQ and found that this entirely abolished darkness-induced inversion (Figure 4C). These results suggest that sGCs (either NO dependent or O_2 dependent) are responsible for synthesizing baseline

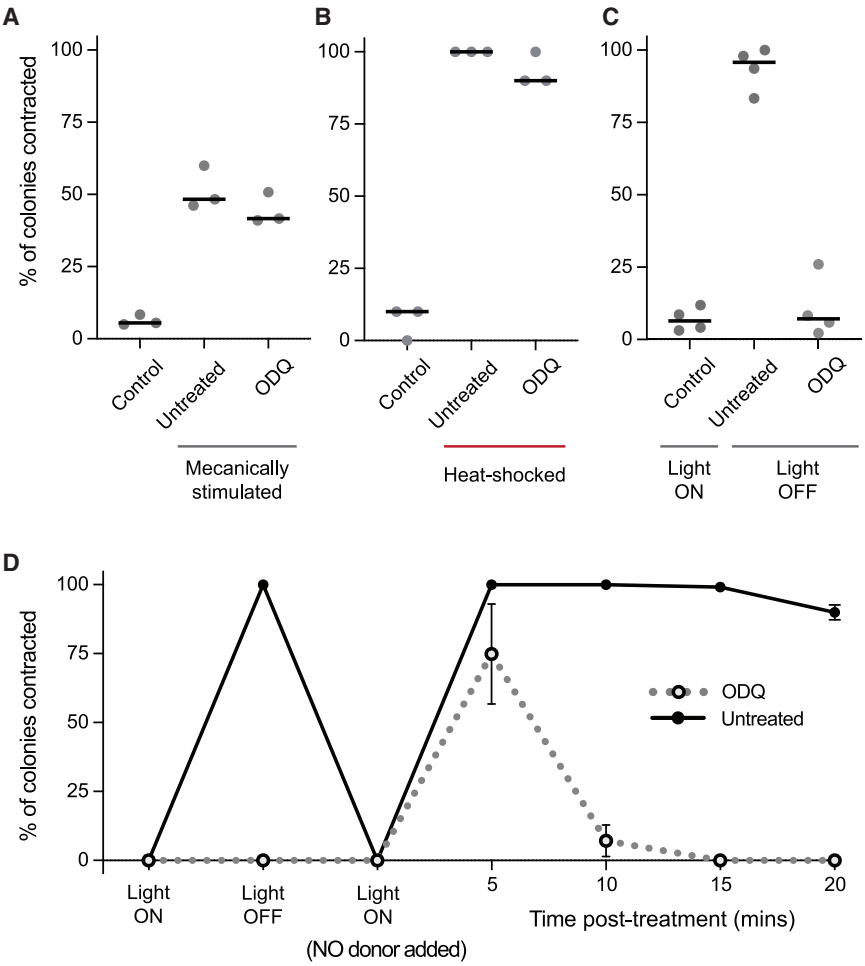

Figure 4. NO/cGMP acts independently of most other inducers of contraction in *C. flexa*

(A and B) Mechanical stimuli and heat shock induce *C. flexa* colony contraction. Inhibition of sGC (50 μM ODQ) did not have an effect on mechanically or heat shock-induced contractions.

(C) Inhibition of sGC (50 μM ODQ) abolished darkness-induced inversion ($p < 0.0001$ by an unpaired t test).

(D) Colonies treated with ODQ did not respond to on/off changes in light but briefly contracted when exposed to NO donor, consistent with earlier results (Figures 3D–3F). Ten min after treatment, ODQ-treated colonies were relaxed, whereas untreated colonies remained contracted for a longer period. In (A–D), each point is the average of n = 3 (A and B) or n = 4 (C and D) biological replicates with at least N = 30 colonies scored per biological replicate. Error bars are standard deviations.

levels of cGMP that are then used during phototransduction. Even though ODQ-treated light-sensitive colonies did not invert in response to darkness, we confirmed that they could still respond to NO by undergoing brief contractions (which were sustained for a much shorter time than in controls; Figure 4D), consistently with earlier results (Figure 3E).

DISCUSSION

Here, we report the presence of NOS, sGCs, and downstream components of NO/cGMP signaling in three choanoflagellate species, at least two of which (*C. flexa* and *C. perplexa*) are capable of collective contractions.[15,47] To our knowledge, this is the first observation of both NOS and sGCs in a nonanimal model. We found that NO causes sustained colony contraction in *C. flexa* and an increase in cGMP concentration in live cells, and that inhibition of sGCs (and thereby reduction in cGMP concentration) accelerated colony relaxation. Moreover, *in vitro* experiments confirmed that NO directly binds *Cf* sGC1, which it activates with a two-step profile in response to different NO concentration, as in animal sGCs.[34]

The observation that colonies treated with the sGC inhibitor initially contracted in response to NO at levels matching untreated colonies, only to relax much more quickly, was unexpected. We hypothesize that NO-induced contractions are mediated through at least two different pathways: a slow pathway (described above) that maintains contraction and requires sGC/cGMP and an (unidentified) fast pathway independent of sGC/cGMP. Moreover, treatment of light-sensitive colonies with the sGC inhibitor abolished darkness-induced contractions (which are known to be mediated by cGMP[15]) but did not prevent NO-induced contractions, further supporting the existence of a second pathway. In other organisms, cGMP-independent NO signaling can involve S-nitrosation, the modification of proteins through the formation of an S–NO covalent bond,[48,49] although the direct targets and functions of S-nitrosation in animals are less well understood than NO/cGMP signaling. It is possible that this mechanism explains the cGMP-independent pathway underlying NO-induced colony contraction in *C. flexa*.

The control of multicellular behavior by NO/cCMP signaling in *C. flexa* is reminiscent of its function in animals, most notably in sponges.[50] In the demosponges *Tethya wilhelma*,[1] *Ephydatia muelleri*,[2] and *Spongilla lacustris*,[3] NO induces global contractions and stops flagellar beating in choanocyte chambers, which interrupts feeding, allows expulsion of clumps of waste, and flushes the aquiferous canal system (a behavior sometimes called "sneezing").[51] Recently, single-cell RNA sequencing in *Spongilla lacustris* revealed that pinacocytes (epithelial cells that cover and shape the sponge body) coexpress NOS and sGC,[3,52] the actomyosin contractility module and the transcription factor serum response factor (Srf), a master regulator of contractility.[3,53,54]

Control of motor and feeding behavior by NO/cGMP is also observed in cnidarians and some bilaterians. In the jellyfish *Aglantha digitale*, NO/cGMP signaling in neurons induces a switch from slow swimming (associated with feeding) to fast swimming (associated with escape) and inhibits tentacular ciliary beating.[11] In the sea pansy (a type of colonial cnidarian) *Renilla koellikeri*, NO/cGMP

increases the amplitude of peristaltic contractions associated with the movement of body fluids through the gastrovascular cavity.[17] Finally, in the nudibranch *Clione limacine* and the snail *Lymnaea stagnalis*, NO activates both feeding and locomotory neural circuits.[55–58] Thus, as in *C. flexa*, the ancient functions of NO/cGMP signaling in animals may include the regulation of feeding and contraction.[16,18,56,59–61] Interestingly, NO signaling also controls metamorphosis in sponges,[7,62] gastropods,[63] annelids,[64] echinoderms,[65,66] and ascidians,[65,67,68] thus regulating a switch from swimming to feeding during irreversible developmental programs. The conservation of the NO-sensitive transduction pathway across choanozoans (including sGC, PKG, CNG, and PDEG; Figure S2C) is consistent with a possible homology of the behavioral response to NO between choanoflagellates and animals. However, the mosaic distribution of eukaryotic and bacterial NOS across choanozoans (Figures 2A and S1A) suggests that the source of NO itself might have switched an unknown number of times during evolution between the ancestral eukaryotic NOS, the horizontally transferred bacterial NOS, and exogenous sources.

In future, identifying the function of *Cf* NOS and *C. flexa* NO- or O_2-selective sGCs will require gene knockout, which is not yet possible in *C. flexa*. Moreover, studies on *Trichoplax* (in which NO/cGMP signaling has been predicted to exist based on genomic data[46]), additional animal phyla, and other choanoflagellates will help flesh out reconstitutions of the early evolution of animal NO signaling.

STAR★METHODS

Detailed methods are provided in the online version of this paper and include the following:

- KEY RESOURCES TABLE
- RESOURCE AVAILABILITY
  - Lead contact
  - Materials availability
  - Data and code availability
- EXPERIMENTAL MODEL AND SUBJECT DETAILS
  - Culture of *Choanoeca flexa*
- METHOD DETAILS
  - Light microscopy—Imaging
  - Compound treatments and colony inversion assays
  - cGMP ELISA
  - NO labeling, imaging, and image analysis
  - Phylogenetic analysis and protein domain identification
  - Construction of expression plasmid
  - Protein expression and purification
  - Analytical size exclusion chromatography
  - Gas ligand binding of bacterial-produced *Cf* sGC1
  - Extinction coefficient of *Cf* sGC1
  - Activity assays and quantification
- QUANTIFICATION AND STATISTICAL ANALYSIS

SUPPLEMENTAL INFORMATION

Supplemental information can be found online at https://doi.org/10.1016/j.cub.2022.04.017.

ACKNOWLEDGMENTS

We thank Flora Rutaganira and Alain Garcia De Las Bayonas for feedback on the manuscript, Daniel J. Richter for sharing the *Ministeria* predicted proteome, and the whole King and Marletta labs for stimulating discussions. This work was supported by an EMBO long-term fellowship (ALTF 1474–2016) to T.B., a Human Frontier Science Program long-term fellowship (000053/2017 L) to T.B., the Institut Pasteur (G5 package; T.B.), the Howard Hughes Medical Institute (N.K.), the National Institute of Health (NIH R01GM127854; M.A.M., Y.W., and B.G.H.G), and the National Science Foundation Graduate Research Fellowship Program (grant no. 1752814; J.R.-R.).

AUTHOR CONTRIBUTIONS

J.R.-R., conceptualization, methodology, validation, formal analysis, investigation, writing – original draft, writing – review & editing, and visualization. Y.W., conceptualization, methodology, validation, formal analysis, investigation, writing – original draft, writing – review & editing, and visualization. B.G.H.G., conceptualization and methodology. M.A.M., conceptualization, methodology, writing – review & editing, supervision, project administration, and funding acquisition. N.K., conceptualization, methodology, writing – review & editing, supervision, project administration, and funding acquisition. T.B., conceptualization, methodology, validation, formal analysis, investigation, writing – original draft, writing – review & editing, supervision, project administration, and funding acquisition.

DECLARATION OF INTERESTS

The authors declare no competing interests.

Received: February 19, 2022
Revised: April 4, 2022
Accepted: April 7, 2022
Published: May 2, 2022

REFERENCES

1. Ellwanger, K., and Nickel, M. (2006). Neuroactive substances specifically modulate rhythmic body contractions in the nerveless metazoon *Tethya wilhelma* (Demospongiae, Porifera). Front. Zool. *3*, 7.
2. Elliott, G.R., and Leys, S.P. (2010). Evidence for glutamate, GABA and NO in coordinating behaviour in the sponge, *Ephydatia muelleri* (Demospongiae, Spongillidae). J. Exp. Biol. *213*, 2310–2321.
3. Musser, J.M., Schippers, K.J., Nickel, M., Mizzon, G., Kohn, A.B., Pape, C., Ronchi, P., Papadopoulos, N., Tarashansky, A.J., Hammel, J.U., et al. (2021). Profiling cellular diversity in sponges informs animal cell type and nervous system evolution. Science *374*, 717–723.
4. Bogdan, C. (2015). Nitric oxide synthase in innate and adaptive immunity: an update. Trends Immunol. *36*, 161–178.
5. Hillyer, J.F., and Estévez-Lao, T.Y. (2010). Nitric oxide is an essential component of the hemocyte-mediated mosquito immune response against bacteria. Dev. Comp. Immunol. *34*, 141–149.
6. Tomankova, S., Abaffy, P., and Sindelka, R. (2017). The role of nitric oxide during embryonic epidermis development of *Xenopus laevis*. Biol. Open *6*, 862–871.
7. Ueda, N., Richards, G.S., Degnan, B.M., Kranz, A., Adamska, M., Croll, R.P., and Degnan, S.M. (2016). An ancient role for nitric oxide in regulating the animal pelagobenthic life cycle: evidence from a marine sponge. Sci. Rep. *6*, 37546.
8. Gibbs, S.M., Becker, A., Hardy, R.W., and Truman, J.W. (2001). Soluble guanylate cyclase is required during development for visual system function in *Drosophila*. J. Neurosci. *21*, 7705–7714.
9. Estephane, D., and Anctil, M. (2010). Retinoic acid and nitric oxide promote cell proliferation and differentially induce neuronal differentiation *in vitro* in the cnidarian *Renilla koellikeri*. Dev. Neurobiol. *70*, 842–852.

10. Pirtle, T.J., and Satterlie, R.A. (2021). Cyclic guanosine monophosphate modulates locomotor acceleration induced by nitric oxide but not serotonin in *Clione limacina* central pattern generator swim interneurons. Integr. Org. Biol. *3*, obaa045.

11. Moroz, L.L., Meech, R.W., Sweedler, J.V., and Mackie, G.O. (2004). Nitric oxide regulates swimming in the jellyfish *Aglantha digitale*. J. Comp. Neurol. *471*, 26–36.

12. Carr, M., Leadbeater, B.S., Hassan, R., Nelson, M., and Baldauf, S.L. (2008). Molecular phylogeny of choanoflagellates, the sister group to Metazoa. Proc. Natl. Acad. Sci. USA *105*, 16641–16646.

13. Denninger, J.W., and Marletta, M.A. (1999). Guanylate cyclase and the .NO/cGMP signaling pathway. Biochim. Biophys. Acta *1411*, 334–350.

14. Andreakis, N., D'Aniello, S., Albalat, R., Patti, F.P., Garcia-Fernàndez, J., Procaccini, G., Sordino, P., and Palumbo, A. (2011). Evolution of the nitric oxide synthase family in metazoans. Mol. Biol. Evol. *28*, 163–179.

15. Brunet, T., Larson, B.T., Linden, T.A., Vermeij, M.J.A., McDonald, K., and King, N. (2019). Light-regulated collective contractility in a multicellular choanoflagellate. Science *366*, 326–334.

16. Colasanti, M., Venturini, G., Merante, A., Musci, G., and Lauro, G.M. (1997). Nitric oxide involvement in Hydra vulgaris very primitive olfactory-like system. J. Neurosci. *17*, 493–499.

17. Anctil, M., Poulain, I., and Pelletier, C. (2005). Nitric oxide modulates peristaltic muscle activity associated with fluid circulation in the sea pansy *Renilla koellikeri*. J. Exp. Biol. *208*, 2005–2017.

18. Colasanti, M., Persichini, T., and Venturini, G. (2010). Nitric oxide pathway in lower metazoans. Nitric Oxide *23*, 94–100.

19. Robertson, H.M. (2009). The choanoflagellate *Monosiga brevicollis* karyotype revealed by the genome sequence: telomere-linked helicase genes resemble those of some fungi. Chromosome Res. *17*, 873–882.

20. Fairclough, S.R., Chen, Z., Kramer, E., Zeng, Q., Young, S., Robertson, H.M., Begovic, E., Richter, D.J., Russ, C., Westbrook, M.J., et al. (2013). Premetazoan genome evolution and the regulation of cell differentiation in the choanoflagellate *Salpingoeca rosetta*. Genome Biol. *14*, R15.

21. Richter, D.J., Fozouni, P., Eisen, M.B., and King, N. (2018). Gene family innovation, conservation and loss on the animal stem lineage. eLife *7*, e34226.

22. Carr, M., Richter, D.J., Fozouni, P., Smith, T.J., Jeuck, A., Leadbeater, B.S.C., and Nitsche, F. (2017). A six-gene phylogeny provides new insights into choanoflagellate evolution. Mol. Phylogenet. Evol. *107*, 166–178.

23. Derbyshire, E.R., and Marletta, M.A. (2009). Biochemistry of soluble guanylate cyclase. Handb. Exp. Pharmacol. 17–31.

24. Horst, B.G., Stewart, E.M., Nazarian, A.A., and Marletta, M.A. (2019). Characterization of a carbon monoxide-activated soluble guanylate cyclase from *Chlamydomonas reinhardtii*. Biochemistry *58*, 2250–2259.

25. Gray, J.M., Karow, D.S., Lu, H., Chang, A.J., Chang, J.S., Ellis, R.E., Marletta, M.A., and Bargmann, C.I. (2004). Oxygen sensation and social feeding mediated by a *C. elegans* guanylate cyclase homologue. Nature *430*, 317–322.

26. Huang, S.H., Rio, D.C., and Marletta, M.A. (2007). Ligand binding and inhibition of an oxygen-sensitive soluble guanylate cyclase, Gyc-88E, from *Drosophila*. Biochemistry *46*, 15115–15122.

27. Cheung, B.H., Arellano-Carbajal, F., Rybicki, I., and de Bono, M. (2004). Soluble guanylate cyclases act in neurons exposed to the body fluid to promote *C. elegans* aggregation behavior. Curr. Biol. *14*, 1105–1111.

28. Boon, E.M., and Marletta, M.A. (2005). Ligand discrimination in soluble guanylate cyclase and the H-NOX family of heme sensor proteins. Curr. Opin. Chem. Biol. *9*, 441–446.

29. Boon, E.M., Huang, S.H., and Marletta, M.A. (2005). A molecular basis for NO selectivity in soluble guanylate cyclase. Nat. Chem. Biol. *1*, 53–59.

30. Cheng, J., He, K., Shen, Z., Zhang, G., Yu, Y., and Hu, J. (2019). Nitric oxide (NO)-releasing macromolecules: rational design and biomedical applications. Front. Chem. *7*, 530.

31. Lord, S.J., Velle, K.B., Mullins, R.D., and Fritz-Laylin, L.K. (2020). SuperPlots: communicating reproducibility and variability in cell biology. J. Cell Biol. *219*, e202001064.

32. Zhao, Y., Brandish, P.E., Di Valentin, M., Schelvis, J.P., Babcock, G.T., and Marletta, M.A. (2000). Inhibition of soluble guanylate cyclase by ODQ. Biochemistry *39*, 10848–10854.

33. Horst, B.G., Yokom, A.L., Rosenberg, D.J., Morris, K.L., Hammel, M., Hurley, J.H., and Marletta, M.A. (2019). Allosteric activation of the nitric oxide receptor soluble guanylate cyclase mapped by cryo-electron microscopy. eLife *8*, e50634.

34. Horst, B.G., and Marletta, M.A. (2018). Physiological activation and deactivation of soluble guanylate cyclase. Nitric Oxide *77*, 65–74.

35. Doyle, M.P., and Duling, B.R. (1997). Acetylcholine induces conducted vasodilation by nitric oxide-dependent and -independent mechanisms. Am. J. Physiol. *272*, H1364–H1371.

36. Sriram, K., Laughlin, J.G., Rangamani, P., and Tartakovsky, D.M. (2016). Shear-induced nitric oxide production by endothelial cells. Biophys. J. *111*, 208–221.

37. Zhang, L., Liu, Q., Yuan, X., Wang, T., Luo, S., Lei, H., and Xia, Y. (2013). Requirement of heat shock protein 70 for inducible nitric oxide synthase induction. Cell. Signal. *25*, 1310–1317.

38. Dulce, R.A., Mayo, V., Rangel, E.B., Balkan, W., and Hare, J.M. (2015). Interaction between neuronal nitric oxide synthase signaling and temperature influences sarcoplasmic reticulum calcium leak: role of nitroso-redox balance. Circ. Res. *116*, 46–55.

39. Rai, K.K., Pandey, N., and Rai, S.P. (2020). Salicylic acid and nitric oxide signaling in plant heat stress. Physiol. Plant. *168*, 241–255.

40. Giovine, M., Pozzolini, M., Favre, A., Bavestrello, G., Cerrano, C., Ottaviani, F., Chiarantini, L., Cerasi, A., Cangiotti, M., Zocchi, E., et al. (2001). Heat stress-activated, calcium-dependent nitric oxide synthase in sponges. Nitric Oxide *5*, 427–431.

41. Leadbeater, B.S. (1983). Distribution and chemistry of microfilaments in choanoflagellates, with special reference to the collar and other tentacle systems. Protistologica *19*, 157–166.

42. James-Clark, H. (1868). XXII.—On the *Spongiæ ciliatæ* as *Infusoria flagellata*; or observations on the structure, animality, and relationship of *Leucosolenia botryoides*. Bowerbank. Ann. Mag. Nat. Hist. *1*, 133–142.

43. Nguyen, N.M., Merle, T., Broders, F., Brunet, A.-C., Sarron, F., Jha, A., et al. (2020). Evolutionary emergence of first animal organisms triggered by environmental mechano-biochemical marine stimulation. Preprint at bioRxiv. https://www.biorxiv.org/content/10.1101/2020.12.03.407668v1.

44. Andrews, G.F. (1897). The living substance as such and as organism. Supplement to. J. Morphol. *XII*.

45. Zhang, X., and Cote, R.H. (2005). CGMP signaling in vertebrate retinal photoreceptor cells. Front. Biosci. *10*, 1191–1204.

46. Moroz, L.L., Romanova, D.Y., Nikitin, M.A., Sohn, D., Kohn, A.B., Neveu, E., Varoqueaux, F., and Fasshauer, D. (2020). The diversification and lineage-specific expansion of nitric oxide signaling in Placozoa: insights in the evolution of gaseous transmission. Sci. Rep. *10*, 13020.

47. Leadbeater, B.S.C. (1983). Life-history and ultrastructure of a new marine species of *Proterospongia* (Choanoflagellida). J. Mar. Biol. Assoc. UK *63*, 135–160.

48. Broniowska, K.A., Diers, A.R., and Hogg, N. (2013). S-nitrosoglutathione. Biochim. Biophys. Acta *1830*, 3173–3181.

49. Smith, B.C., and Marletta, M.A. (2012). Mechanisms of S-nitrosothiol formation and selectivity in nitric oxide signaling. Curr. Opin. Chem. Biol. *16*, 498–506.

50. Simion, P., Philippe, H., Baurain, D., Jager, M., Richter, D.J., Di Franco, A., Roure, B., Satoh, N., Quéinnec, É., Ereskovsky, A., et al. (2017). A large and consistent phylogenomic dataset supports sponges as the sister group to all other animals. Curr. Biol. *27*, 958–967.

51. Elliott, G.R., and Leys, S.P. (2007). Coordinated contractions effectively expel water from the aquiferous system of a freshwater sponge. J. Exp. Biol. *210*, 3736–3748.

52. Nickel, M., Scheer, C., Hammel, J.U., Herzen, J., and Beckmann, F. (2011). The contractile sponge epithelium *sensu lato* – body contraction of the demosponge *Tethya wilhelma* is mediated by the pinacoderm. J. Exp. Biol. *214*, 1692–1698.

53. Miano, J.M., Long, X., and Fujiwara, K. (2007). Serum response factor: master regulator of the actin cytoskeleton and contractile apparatus. Am. J. Physiol. Cell Physiol. *292*, C70–C81.

54. Brunet, T., Fischer, A.H., Steinmetz, P.R., Lauri, A., Bertucci, P., and Arendt, D. (2016). The evolutionary origin of bilaterian smooth and striated myocytes. eLife *5*, e1960.

55. Moroz, L.L., Norekian, T.P., Pirtle, T.J., Robertson, K.J., and Satterlie, R.A. (2000). Distribution of NADPH-diaphorase reactivity and effects of nitric oxide on feeding and locomotory circuitry in the pteropod mollusc, *Clione limacina*. J. Comp. Neurol. *427*, 274–284.

56. Moroz, L.L., and Kohn, A.B. (2011). Parallel evolution of nitric oxide signaling: diversity of synthesis and memory pathways. Front. Biosci. (Landmark Ed.) *16*, 2008–2051.

57. Moroz, L.L., Park, J.H., and Winlow, W. (1993). Nitric oxide activates buccal motor patterns in *Lymnaea stagna*lis. NeuroReport *4*, 643–646.

58. Kobayashi, S., Sadamoto, H., Ogawa, H., Kitamura, Y., Oka, K., Tanishita, K., and Ito, E. (2000). Nitric oxide generation around buccal ganglia accompanying feeding behavior in the pond snail, *Lymnaea stagnalis*. Neurosci. Res. *38*, 27–34.

59. Yabumoto, T., Takanashi, F., Kirino, Y., and Watanabe, S. (2008). Nitric oxide is involved in appetitive but not aversive olfactory learning in the land mollusk *Limax valentianus*. Learn. Mem. *15*, 229–232.

60. Cristino, L., Guglielmotti, V., Cotugno, A., Musio, C., and Santillo, S. (2008). Nitric oxide signaling pathways at neural level in invertebrates: functional implications in cnidarians. Brain Res. *1225*, 17–25.

61. Jacklet, J.W. (1997). Nitric oxide signaling in invertebrates. Invert. Neurosci. *3*, 1–14.

62. Song, H., Hewitt, O.H., and Degnan, S.M. (2021). Arginine biosynthesis by a bacterial symbiont enables nitric oxide production and facilitates larval settlement in the marine-sponge host. Curr. Biol. *31*. 433.e3–437.e3.

63. Froggett, S.J., and Leise, E.M. (1999). Metamorphosis in the marine snail Ilyanassa obsoleta, yes or NO? Biol. Bull. *196*, 57–62.

64. Biggers, W.J., Pires, A., Pechenik, J.A., Johns, E., Patel, P., Polson, T., and Polson, J. (2012). Inhibitors of nitric oxide synthase induce larval settlement and metamorphosis of the polychaete annelid *Capitella teleta*. Invertebr. Reprod. Dev. *56*, 1–13.

65. Bishop, C.D., and Brandhorst, B.P. (2003). On nitric oxide signaling, metamorphosis, and the evolution of biphasic life cycles. Evol. Dev. *5*, 542–550.

66. Bishop, C.D., and Brandhorst, B.P. (2007). Development of nitric oxide synthase-defined neurons in the sea urchin larval ciliary band and evidence for a chemosensory function during metamorphosis. Dev. Dyn. *236*, 1535–1546.

67. Ueda, N., and Degnan, S.M. (2013). Nitric oxide acts as a positive regulator to induce metamorphosis of the ascidian *Herdmania momus*. PLoS One *8*, e72797.

68. Comes, S., Locascio, A., Silvestre, F., d'Ischia, M., Russo, G.L., Tosti, E., Branno, M., and Palumbo, A. (2007). Regulatory roles of nitric oxide during larval development and metamorphosis in *Ciona intestinalis*. Dev. Biol. *306*, 772–784.

69. Torruella, G., de Mendoza, A., Grau-Bové, X., Antó, M., Chaplin, M.A., del Campo, J., Eme, L., Pérez-Cordón, G., Whipps, C.M., Nichols, K.M., et al. (2015). Phylogenomics reveals convergent evolution of lifestyles in close relatives of animals and fungi. Curr. Biol. *25*, 2404–2410.

70. Dereeper, A., Guignon, V., Blanc, G., Audic, S., Buffet, S., Chevenet, F., Dufayard, J.F., Guindon, S., Lefort, V., Lescot, M., et al. (2008). Phylogeny.fr: robust phylogenetic analysis for the non-specialist. Nucleic Acids Res. *36*, W465–W469.

71. Letunic, I., and Bork, P. (2021). Interactive Tree Of Life (iTOL) v5: an online tool for phylogenetic tree display and annotation. Nucleic Acids Res. *49*, W293–W296.

72. Barr, I., and Guo, F. (2015). Pyridine hemochromagen assay for determining the concentration of heme in purified protein solutions. Bio Protoc. *5*, e1594.

STAR★METHODS

KEY RESOURCES TABLE

REAGENT or RESOURCE	SOURCE	IDENTIFIER
Bacterial and virus strains		
Escherichia coli BL21 Star (DE3)	UC Berkeley QB3 Macrolab	N/A
Escherichia coli DH10b-T1R	Prepared in-house	N/A
Biological samples		
Choanoeca flexa	Our lab, isolated from Curaçao splash pool	https://doi.org/10.1126/science.aay2346
Chemicals, peptides, and recombinant proteins		
ODQ	BioVision	2051
proliNONOate	Cayman Chemical Company	82145
DEANONOate	Cayman Chemical Company	82100
DAF-FM	Invitrogen	D-23844
DL-Proline	Sigma Aldrich	609-36-9
poly-D-lysine	Sigma Aldrich	P6407
16% paraformaldehyde	Fisher Scientific	50-980-487
Guanosine-5'-triphosphate, sodium salt hydrate	Sigma Aldrich	36051-31-7
Sodium dithionite	Sigma Aldrich	7775-14-6
DL-dithio-1,4-threitol	BACHEM	3483-12-3
Magnesium chloride hexahydrate	MP Biomedicals	7791-18-6
Pyridine	Sigma Aldrich	110-86-1
Potassium ferricyanide	Mallinckrodt Pharmaceuticals	13746-66-2
Precision Plus Protein Standard, unstained	BioRad	161-0363
Critical commercial assays		
ENZO Direct cGMP ELISA kit	Enzo Life Sciences	ADI-900-014
ENZO cGMP ELISA kit, extracellular	Enzo Life Sciences	ADI-901-013
Deposited data		
Cf NOS	GeneBank	ON075806
Cf sGC1	GeneBank	ON075810
Cf sGC2	GeneBank	ON075809
Cf sGC3	GeneBank	ON075808
Cf sGC4	GeneBank	ON075807
Oligonucleotides		
pYW5 Forward: TAAGAAGGAGATATACCA TG TATGGCTTGGTGCACGAAGC	This Paper	N/A
pYW5 Reverse: TAATGGTGATGATGGTGA TG AACTATAGTCTGCTTGCCAACG	This Paper	N/A
Recombinant DNA		
pYW5 (*Cf* sGC1 in pET28b backbone)	This paper	N/A
pGro7 (GroEL/GroES)	Takara Bio	3340
Software and algorithms		
ImageJ version 2.3.0	ImageJ Software Analysis	https://imagej.nih.gov/ij/index.html
PRISM version 9.0.0	GraphPad	https://www.graphpad.com/
Other		
Agilent Technologies Cary 300 UV-vis Spectrophotometer	Agilent Technologies	10071600
Nanodrop 2000 Microvolume Spectrophotometer	Thermo Scientific	ND-2000

(*Continued on next page*)

Continued

REAGENT or RESOURCE	SOURCE	IDENTIFIER
AKTA Purifier UPC 100 FPLC System	GE Healthcare	10475
POROS HQ20 10x100mm Anion Exchange Column	Applied Biosystems	1232907
Superdex 200 increase 10/300 GL Size Exclusion Column	GE Healthcare	GE28-9909-44
Zeba Spin Desalting Column	Thermo Scientific	89882
His60 Ni Superflow Resin	Takara Bio	635677
SpectraMax M3 plate reader	Molecular Devices	89429-536

RESOURCE AVAILABILITY

Lead contact

Further information and requests for resources and reagents should be directed to and will be fulfilled by the lead contact, Thibaut Brunet (thibaut.brunet@pasteur.fr).

Materials availability

This study did not generate new unique reagents.

Data and code availability

All NOS and sGC sequences from *C. flexa* were deposited onto GenBank (accession numbers below). All other data reported in this paper will be shared by lead contact upon request. This paper does not report original code. Any additional information required to reanalyze the data reported in this paper is available from the lead contact upon request.

EXPERIMENTAL MODEL AND SUBJECT DETAILS

Culture of *Choanoeca flexa*

Colonies were cultured in 1% to 15% Cereal Grass Medium (CGM3) in artificial seawater (ASW). Polyxenic cultures (continuously passaged from a previously described environmental isolate[15]) were maintained at 22°C under a light-dark cycle of 12:12 hours in a Caron low temperature incubator equipped with a lamp (Venoya Full Spectrum 150W Plant Growth LED) controlled by a programmable timer (Leviton VPT24^{-1}PZ Vizia). Polyxenic cultures used in most experiments were not light-sensitive, possibly due to progressive loss of bacterial diversity during serial passaging (as bacterially provided retinal is known to be required for photosensation in *C. flexa*[15]). Light-sensitive sheets used in photosensation experiments (Figures 4C and 4D) were thawed from stocks that had been frozen immediately after clonal isolation from a Curaçao isolate and cultured as described above.

METHOD DETAILS

Light microscopy—Imaging

Colonies were imaged in FluoroDishes (World Precision Instruments FD35-100) by differential interference contrast (DIC) microscopy using a 20x Zeiss objective mounted on a Zeiss Observer Z.1 with Hamamatsu Orca Flash 4.0 V2 CMOS camera (C1140-22CU).

Compound treatments and colony inversion assays

Small molecule inhibitor treatments and colony inversion assays were performed in 24-well plates (Fisher Scientific 09-761-146) containing 1 mL *C. flexa* culture per well. ODQ (pan-soluble guanylate cyclase inhibitor, BioVision 2051) was added 1 hour before behavioral assays. Addition of each small molecule compound was followed by a gentle swirl of the 24-well plate to ensure mixing. For each assay, all colonies visible within a well were counted (at least 30 colonies per biological replicate). All behavioral experiments were conducted under ambient light in the laboratory, unless indicated otherwise.

NO donor-induced inversion

The NO donors proliNONOate (Cayman Chemical Company 82145) and DEANONOate (Cayman Chemical Company 82100) were dissolved according to provider's instructions and stored as single-use aliquots at -80°C. Addition of NO donor proliNONOate induced inversion within 1-2 minutes. Prior to counting, colonies were fixed by addition of 16% ice-cold PFA in a 1:3 volumetric ratio, resulting in a final concentration of 4% PFA. Contracted and relaxed colonies were then manually counted by observation under a Leica DMIL LED transmitted light microscope.

Light-induced sheet inversion

After treatment with small molecule compounds, light-to-dark transitions were performed by manually switching off the light source of the DMIL LED microscope. The "light off" condition lasted for one minute before sheets were fixed and scored as described above.

Mechanically induced sheet inversion

3 mL of *C. flexa* culture were transferred to T12.5 culture flasks (Fisher Scientific 353107) and mechanically stimulated by vortexing on a Vortex Genie 2 (Scientific industries) on "Slow" setting for 5 seconds. Sheets were immediately fixed and scored as above.

Heat shock-induced sheet inversion

Colonies in 24-well plates were treated with inhibitors as described above and placed at the surface of a 37°C warm bath for one minute. Sheets were immediately fixed and scored as above.

cGMP ELISA

For *in vivo* quantification of cGMP was performed with an ENZO Direct cGMP ELISA kit (ADI-900-014, 96 wells) as directed by the manufacturer. For each biological replicate, 90 mL of dense (>10^6 cells/mL) *C. flexa* culture was centrifuged for 5 minutes at 3000 x g and resuspended in 25 mL of ASW to wash the bacteria away. After the third wash, the cells were resuspended in 200 μL of ASW and split into one control (100 μL) and one treated sample (100 μL). The samples were lysed and quantified in parallel in each assay. Colonies from the "NO donor" group were treated with 0.25 μM proliNONOate 5 minutes before lysis. Values were read on a SpectraMax M3 plate reader (Molecular Devices).

NO labeling, imaging, and image analysis

C. flexa cultures were transferred into 15 mL Falcon tubes and vortexed in "fast" setting on a Vortex Genie 2 for one minute to dissociate colonies into single cells. Cells were washed 3 times with artificial seawater (ASW) by centrifuging them for 5 minutes at 3000 x g and resuspending them in 25 mL of ASW. After the last wash, cells were resuspended in 1.5 mL ASW and transferred into a 1.5 mL Eppendorf tube. Cells were incubated in 10 μM DAF-FM (Invitrogen, D-23844) for 1 hour and rinsed twice with ASW to wash away the unincorporated dye. Cells were then transferred into a FluoroDish charged with a Corona surface treater and coated with poly-D-lysine, following a previously published protocol.[15] We let the cells adhere to the bottom of the dish for 30 minutes before imaging on a Z.1 Zeiss Imager with a Hamamatsu Orca Flash 4.0 V2 CMOS camera (C11440-22CU) and a 40x water immersion objective (C-Apochromat, 1.1 NA) for DIC and green epifluorescence imaging with a frame rate of 1 frame per minute. The NO donors (0.25 μM proliNONOate or 0.5 μM DEANONOate) were added 5 minutes after imaging began. We quantified intracellular fluorescence intensity using ImageJ. Change in fluorescence intensity was calculated by subtracting the fluorescence intensity at minute 1 from fluorescence intensity at minute 30.

Phylogenetic analysis and protein domain identification

We screened a selection of fully sequenced genomes for homologs of sGC and NOS with the following strategy: the protein sequences of *Homo sapiens* sGC-α1 and brain nitric oxide synthase (NOS1) were used as BLASTp queries against the NCBI database restricted to the following list of species:

- Eukaryotes: *Homo sapiens* (Hsa), *Branchiostoma floridae* (Bfl), *Drosophila melanogaster* (Dme), *Capitella teleta* (Cte), *Nematostella vectensis* (Nve), *Amphimedon queeslandica* (Amq), *Mnemiopsis leidyi, Trichoplax adhaerens* (Tadh), *Salpingoeca rosetta* (Sro), *Capsaspora owczarzaki, Sphaereoforma arctica* (Sphac), *Abeoforma whisleri, Creolimax fragrantissima, Pirum gemmata, Aspergillus oryzae* (Asory), *Jimgerdemannia flammicorona* (Jifla), *Rhizoctonia solani* (Rhiso), *Pterula gracilis* (Ptegra), *Schizosaccharomyces pombe, Tuber melanosporum, Cryptococcus neoformans, Ustilago maydis, Cryptococcus neoformans, Ustilago maydis, Rhizopus oryzae, Allomyces macrogynus, Batrachochytrium dendrobatidis, Spizellomyces punctatus, Thecamonas trahens, Dictyostelium discoideum, Polysphondylium pallidum, Entamoeba histolytica, Arabidopsis thaliana, Selaginella moellendorffii, Physcomitrella patens, Chlamydomonas reinhardtii, Volvox carteri* (Vcar), *Chlorella variabilis* (Chl), *Ostreococcus tauri* (Ostau), *Ectocarpus siliculosus, Phaeodactylum tricornutum, Thalassiossira pseudonana, Phytophthora infestans, Toxoplasma gondii, Tetrahymena thermophila, Perkinsus marinus, Guillardia theta, Naegleria gruberi* (Ngru), *Trypanosoma cruzi, Leishmania major, Trichomonas vaginalis, Giardia lamblia, Bigelowiella natans, Emiliania huxleyi*
- Archaea: *Nanoarchaeum equitans, Ignicoccus islandicus, Natronolimnobius baerhuensis, Halorientalis regularis, Halostagnicola kamekurae, Halalkalicoccus subterraneus, Halobiforma nitratireducens* (Halob), *Natronobacterium gregoryi* (Natr), *Haloplanus natans, Halovenus aranensis* (Halar), *Halonotius pteroides* (Halo)
- Bacteria: *Actinocrispum wychmicini* (Actin), *Kibdelosporangium aridum* (Kibd), *Crossiella equi* (Cross), *Lentzea xinjiangensis* (Lentz)*Nocardioides speluncae* (Noc), *Saccharopolyspora spinosa* (Sspi), *Synechococcus sp. PCC 7335* (Syn), *Nostoc cycadae* (Nocyc), *Anabaenopsis circularis* (Ancir), *Planktothrix paucivesiculata* (Plank), *Crinalium epipsammum* (Crinep), *Spirosoma radiotolerans* (Spiro), *Roseinatronobacter monicus* (Rose)

Additional BLASTp searches were conducted against a published dataset of 19 choanoflagellate transcriptomes,[21] the *C. flexa* transcriptome[15], the *Mnemiopsis leidyi* genome (https://research.nhgri.nih.gov/mnemiopsis/sequenceserver/) and the *Ministeria vibrans* transcriptome[69] (and courtesy of Daniel J. Richter). The *C. flexa* NOS and sGC predicted protein sequences were deposited onto NCBI with the following accession numbers: GenBank: ON075806 (for *Cf* NOS), GenBank: ON075810 (for *Cf* sGC1), GenBank: ON075809 (for *Cf* sGC2), GenBank: ON075808 (for *Cf* sGC3), and GenBank: ON075807 (for *Cf* sGC4).

Domain architectures were predicted using the CD-search tool from NCBI. For phylogenetic reconstructions, sequences were aligned using Clustal implemented in Geneious Prime (2021 version). The NOS sequence alignment was manually trimmed to be restricted to the

oxygenase domain and the sGC alignment was trimmed using Gblocks with minimally stringent parameters. Phylogenetic trees were reconstructed using PhyML and BMGE implemented on http://phylogeny.lirmm.fr/phylo_cgi/index.cgi.[70] Trees were visualized using iTOL (https://itol.embl.de/)[71] and further edited in Adobe Illustrator 2021. Species silhouettes were added from PhyloPic (http://phylopic.org/).

Construction of expression plasmid

First-strand *C. flexa* cDNA (extracted as in[15]) was used as the template for cloning *Cf* sGC1. Forward and reverse primers were designed against 5' and 3' ends of the target transcript (transcript name: TRINITY_DN6618_c0_g1_i1 in the published transcriptome[15]). Forward: TAAGAAGGAGATATACCATG TATGGCTTGGTGCACGAAGC; reverse: TAATGGTGATGATGGTGATG AACTATAGTCTG CTTGCCAACG. Underlined portions anneal to the sequence template. The PCR product was inserted into a pET28b vector using Gibson assembly, and the cloning product was verified by sequencing (UC Berkeley sequencing facility).

Protein expression and purification

pET_*Cf* sGC1 was transformed into *E. coli* BL21star (DE3) cells co-expressing the chaperone GroEL/ES from the pGro7 plasmid (Takara Biosciences). After overnight incubation at 37 °C in LB Miller media supplemented with 50 μg/mL kanamycin, 20 μg/mL chloramphenicol and 500 μM iron (III) chloride, cells were subcultured 1:200 into TB media supplemented with 50 μg/mL kanamycin, 20 μg/mL chloramphenicol, 500 μM iron (III) chloride, 0.5 mg/mL L-arabinose, and 2 mg/mL glucose, grown at 37 °C. Once cell density reached OD_{600} = 0.6, 1 mM 5-aminolevulinic acid was added to the culture, and culturing temperature was lowered to 18 °C. After 15 minutes of incubation, protein production was induced by addition of 500 μM isopropyl β-D-1-thiogalactopyranoside and cultures were incubated for an additional 18 hours. Cell culture was harvested by centrifuging at 4200 g for 25 min. Cells were collected, flash frozen in liquid nitrogen, and stored at -80 °C until purification.

All protein purification steps were done at 4 °C unless otherwise noted. Cells were resuspended in equal volume of buffer A (50 mM sodium phosphate, 150 mM NaCl, 5 mM imidazole, 5% glycerol, pH 8.0) supplemented with 110 mM benzamidine, 0.4 mM AEBSF, and 0.3 mg/mL DNase. Cell resuspension was lysed using an Avestin EmulsiFlex-C5 homogenizer. Cell lysate was collected and clarified by centrifugation at 32,913 g for 55 min, and the supernatant was collected and loaded onto a His60 Ni Superflow gravity column (Takara Bio). The column was washed twice, first with 10 CV buffer A, and then with 10 CV of a 9:1 mixture of buffer A and buffer B (50 mM sodium phosphate, 150 mM NaCl, 400 mM imidazole, 5% glycerol, pH 8.0). Protein was eluted with 5 CV buffer B in 1 mL fractions. Fractions with heme absorbance were pooled and concentrated using a 50 kDa cutoff spin concentrator and supplemented with 5 mM DTT and 1 mM EDTA for overnight storage. Subsequently, protein was passed over a POROS HQ2 anion exchange column (Applied Biosystems). After loading, the column was washed with 5 CV of buffer C (25 mM triethanolamine, 25 mM NaCl, 5 mM DTT, pH 7.4) and developed over a gradient of 100 mM – 300 mM NaCl over 17 CV. The protein absorption spectrum was measured using a Nanodrop 2000 microvolume spectrophotometer (ThermoFisher Scientific). Subsequently, protein was aliquoted, flash frozen in liquid nitrogen, and stored at -80 °C for future use.

Analytical size exclusion chromatography

Purified *Cf* sGC1 and the protein standard mixture were injected onto a Superdex 200 Increase 10/300 GL column (GE healthcare) equilibrated with buffer F (50 mM triethanolamine, 150 mM NaCl, 5 mM DTT, 5% glycerol). Protein elution was monitored by UV absorbance at 280 nm.

Gas ligand binding of bacterial-produced *Cf* sGC1

Cf sGC1 was handled in an argon-filled glove bag. Protein-bound heme was reduced by adding sodium dithionite (~500-fold excess over the protein conc.). Excess dithionite was removed by gel filtration of the protein into Buffer E (50 mM HEPES, 150 mM NaCl, 5% glycerol, pH 7.4) using a pre-equilibrated Zeba spin desalting column. A ferrous, ligand-free UV-vis absorption spectrum was collected on a Cary 300 UV-vis Spectrophotometer. Fe(II)-NO bound *Cf* sGC1 was generated by adding the NO-releasing molecule proliNONOate (~10-fold excess) to the protein sample, and Fe(II)-CO bound *Cf* sGC1 was generated by adding CO-sparged Buffer E to the protein sample before collecting a spectrum.

Extinction coefficient of *Cf* sGC1

The extinction coefficient of the Soret maximum of reduced *Cf* sGC1 was measured using two assays performed in tandem: heme concentration in a sample of *Cf* sGC1 was determined using pyridine hemochromagen assay, and the heme Soret absorption of the protein sample was measured using UV-vis spectroscopy as described above. The pyridine hemochromagen assay was carried out following a reported protocol.[72] Briefly, a reduced protein sample with a known Soret band absorbance was diluted 5-fold in Buffer E, and then further diluted 2-fold in Solution I (0.2 M NaOH, 40% pyridine, 500 μM potassium ferricyanide) to yield the oxidized pyridine hemochromagen. An aliquot (10 μL) of Solution III (0.5 M sodium dithionite, 0.5 mM NaOH) was then added to the oxidized pyridine hemochromagen sample to yield the reduced pyridine hemochromagen. The UV-vis absorption spectrum of the reduced pyridine hemochromagen was measured on a Cary 300 UV-vis spectrophotometer. Absorption at 557 nm(ε = 34,700 $mM^{-1}cm^{-1}$) was used to calculate the heme concentration in the pre-dilution sample, and the extinction coefficient of the heme cofactor of *Cf* sGC1 was calculated by dividing the reduced heme absorption by the heme concentration.

Activity assays and quantification

Specific activity for *Cf* sGC1 was measured by quantifying the amount of cGMP produced in duplicate end-point activity assays, done in biological triplicate. *Cf* sGC1 from previously frozen aliquots was thawed and reduced in an anaerobic chamber as described above. The reduced protein was used without further treatment for the basal (unliganded) activity assay. A UV-vis spectrum for the unliganded sample was obtained using a Nanodrop 2000 microvolume spectrophotometer, and the Soret maximum was used to quantify heme-bound protein concentration (ε_{428} = 101,000 $M^{-1}cm^{-1}$). Only protein with a Soret:280 ratio > 1 was used for activity assays. To the remaining reduced protein, proliNONOate was added to a final concentration of 400 μM by the addition of 1 μL of a stock solution of 10 mM proliNONOate in 10 mM NaOH, and the protein sample was incubated at 4 °C for 5 min to yield the xsNO sample. The xsNO-bound UV-vis spectrum was then collected. The protein concentration of the xsNO sample was assumed to be the same as the unliganded sample. The xsNO sample was then buffer exchanged by gel filtration using a Zeba spin column into buffer E to yield the 1-NO sample, and the UV-vis spectrum was collected. The concentration of the 1-NO sample was calculated based on the NO-bound Soret absorbance at 399 nm compared to that of the xsNO sample. Activity assays were carried out at 25 °C in Buffer E supplemented with 5 mM DTT and 3 mM $MgCl_2$ with *Cf* sGC1 concentration at 40 nM. To obtain the xsNO state, 70 μM proliNONOate was added. The reaction was initiated by addition of 1.5 mM GTP, and timepoints were quenched by diluting the reaction mixture 1:4 to a solution of 125 mM zinc acetate, and pH adjusted by adding equal volume of 125 mM sodium carbonate. Assay samples were stored at -80 °C until analyzed. Quenched assay samples were thawed at room temperature, centrifuged at 21,130 x g at 4 °C to remove zinc precipitate. Supernatant was collected and diluted 250-fold for the analysis. cGMP content of each assay sample was quantified in duplicate using an enzyme-linked immunosorbent assay (Enzo Life Sciences) following the manufacturer's protocol. Initial rate of the reaction was calculated using the linear phase of the time course, where <10% of substrate has been depleted.

QUANTIFICATION AND STATISTICAL ANALYSIS

Information about the quantification and statistical details of experiments can be found in the corresponding figure legends. Statistical tests and graphs were produced using Prism 9.0.0.